Available online at www.sciencedirect.com
SCIENCE DIRECT®
ELSEVIER
Computer Communications xx (xxxx) 1–20
computer communications
www.elsevier.com/locate/comcom

A study of H.263 traffic modeling in multipoint videoconference sessions over IP networks

A. Drigas[a], S. Kouremenos[a,b,*], Y. Bakopoulos[a], V. Loumos[b]

[a]*Department of Technological Applications, National Center for Scientific Research 'DEMOKRITOS', P.O. Box 15310, Gr. Ag. Paraskevi Attikis, Greece*
[b]*School of Electrical and Computer Engineering, National Technical University of Athens, P.O. Box 15780, Gr. Zographou, Attikis, Greece*

Received 2 March 2004; revised 16 March 2005; accepted 16 March 2005

Abstract

This manuscript is a contribution on the modeling of H.263 traffic in multipoint videoconference sessions over IP Networks. Our study includes analysis and modeling assessment of extensive data gathered during realistic videoconference sessions between commercial H.263-compliant terminal clients (with different videoconference software packages installed). All terminal clients were communicating through a Multipoint Control Unit (software or hardware MCU) at 'switched presence' mode and for comparative purposes the same typical videoconference content (a person speaking, with mild movement and occasional zoom/span) was used. The analysis of the H.263 data at the frame level suggests that the traffic from the different terminals to the MCU can be represented by a stationary stochastic process with an AutoCorrelation Function (ACF) rapidly decaying to zero and a Gamma formed marginal frame-size Probability Distribution Function (PDF). An accurate analysis of the H.263 traffic from all terminals (with the same visual content and different videoconference software used) shows indicative differences in the ACF and PDF of different terminals' traffic and insights that no generic traffic model can be applied for all cases. Aiming at a realistic, reusable and simple H.263 traffic model, conservative enough for queueing analysis and network estimation, this study discusses methods for calculating the appropriate model parameters from the observed traffic data and proposes a new technique for unconventional fitting of the PDF. The presented modeling and queueing results indicate the suitability of the proposed models for H.263 traffic modeling in IP networks.

Keywords: H.263 traffic modeling; Multipoint videoconference; MCU; Queueing

1. Introduction

Videoconference traffic modeling has been extensively studied in literature and as a result a wide range of methods (linear and non-linear) can be found. Successful traffic modeling can provide valuable insights about the resulting network load and enables a theoretical assessment of the network performance. However, the variation of the videoconference session parameters (number of participants, video bit rate, frame rate) and visual contents as well as the differences in the implementations of the video coding algorithms turn accurate video traffic modeling into a complex procedure.

The results of earlier studies as [2,3,16,19,21], concerning variable bit-rate video streams in ATM networks, indicate that the histogram of the vbr video frame sizes exhibits an asymmetric and of Gamma form shape and that the autocorrelation function decays quickly (approximately exponentially) to zero. An important body of knowledge in vbr traffic modeling is the approach in [13] where the DAR(1) [9] model is introduced. In this study, the authors noted that AR models of at least order two are required for a satisfactory modelling of the examined H.261 encoded traffic patterns. However, in the same study, the authors observed that a simple DAR(1) model, based on a discrete-time, discrete state Markov Chain performs better—with respect to queueing—than a simple AR(2) model. In the same study, the parameters of the DAR(1) model were matched to the frame-size sequence histogram (fitted to a Gamma probability distribution function by the method of

* Corresponding author. Address: Department of Technological Applications, National Center for Scientific Research 'DEMOKRITOS', P.O. Box 15310, Gr. Ag. Paraskevi Attikis, Greece. Tel.: +30 210 6503143; fax: +30 210 6532910.
E-mail address: skourem@central.ntua.gr (S. Kouremenos).

0140-3664/$ - see front matter © 2005 Elsevier B.V. All rights reserved.
doi:10.1016/j.comcom.2005.03.007

moments) and the exponential autocorrelation decay rate (derived from the AR(2) model). Several other models have been proposed for vbr video traffic modeling such as the GBAR(1) [5] and the SCENIC model [6]. The GBAR model could be a solution for H.263 traffic modeling, as it was especially designed for videoconference and its performance with respect to queueing was found to be similar to DAR(1). On the contrary, SCENIC is oriented to full motion video and not to a typical videoconference content with no abrupt scene changes.

Newer studies of vbr video traffic modeling reinforce the general conclusions obtained by the above earlier studies, by evaluating and extending the existing models and also proposing new methods for successful and accurate modeling. Of particular importance for our work, is the approach in [23] where a continuous version of DAR(1) model was proposed, named C-DAR(1). The C-DAR(1) model combines an approach utilizing a discrete-time Markov chain with a continuous-time Markov chain. The C-DAR(1) model is suitable for theoretical analysis using the fluid flow method [27]. Furthermore, in [20], a 'stuffing' method was used for grouping frames into variable frame periods. In this study, the use of movies, like Starwars, as visual content, led to frames generation with an approximate Gamma PDF (more complex when a target rate was imposed) and an ACF quickly decaying to zero. In [10], H.263+coded vbr video traffic in ATM networks was studied and the authors proposed a new model called DAR(M) which is a compound DAR(1) model. The DAR(M) model analyses the number of cells in each type of macroblock (MB) of a frame separately (I-coded, P-coded and N-coded). The final model is the mean of the DAR(1) models for each type of MB. For the purpose of PDF modeling and correlation coefficients estimation (in the same study), the authors used the typical methods of DAR(1). A scene-based MPEG traffic modeling was proposed in [17]. In this study, the authors used a simple scene detection algorithm that models scene changes by a state transition matrix and the number of GOPs of a scene by a geometric distribution. A shifting level process was applied in [18] to capture the Long Range Behavior of vbr video traffic. In this study, the authors proposed a compound ACF consisting of an exponential function, in the small lag, and a hyperbolic function in the large lag region. Long range dependence, however, is an issue of no interest here as videoconference traffic has been found to be only asymptotically self-similar [7], at a time scale not affecting queueing. This fact makes the short-range dependent method of DAR(1) and extensions of it appropriate for H.263 traffic modeling. Furthermore, a study of measurement and simulation of videoconference traffic (H.261 and H.263) in [4] indicated the influence of the session parameters (codec, quality, frame rate, maximum bandwidth) on the generated traffic pattern. Again, the PDF of H.263 traffic (at the frame level) was found to be of Gamma form and the ACF was decaying quickly to zero. A normal mixture distribution for vbr video traffic was proposed in [11] instead of the Gamma–Pareto distribution that was claimed to perform better than the simple Gamma and lognormal distributions (although it is rather complex). Towards the modelling of videoconference traffic encoded by the ViC Intra-H261 encoder, the author in [26] proposed a DAR(p) model using the Weibull instead of the Gamma density for the fit of the sample histogram.

Relevant recent studies are also [14] and [15]. In [14], the authors proposed a new marginal matching technique that produces a generalized model better than the GBAR and other DAR models. An AR-based analysis is performed in [15] for the modeling of MPEG video at GOP layer in ATM packet switching networks. GOP-based models proposed were tested with movies (like Star Wars) and seemed to perform satisfactorily.

Today, a large number of videoconference platforms exist, the majority of them over IP-based networking infrastructures and using practical implementations of the H.263 standard [8] for video coding. H.263[1] is extensively used because of its suitability for transmission over low bandwidth pipes (ADSL, ISDN) and its low processing demands (applicable to hand-held devices). In comparison to the previous implementation of ITU, H.261, it is generally confirmed and experimentally proved [4] that the H.263 encoder is intended to be used on links with smaller capacity (less than 64 Kbps) and thus produces frames which are in the average shorter than the frames generated by H.261 applications. Moreover, concerning the H.263 video codec, there are several problems of interoperability, due to the existence of different coding 'flavors'. There are H.263 draft, H.263 final and H.263+ implementations. This being the case, it is of great importance to know whether the models established in literature (for H.261, H.263 and vbr video traffic modeling) are appropriate for traffic modeling of the various implementations of the H.263 coding algorithm. It is a point of question whether all the existing H.263 versions generate similar traffic so that a common model could be applied. If not, new or alternative models should be proposed for each case. Moreover, videoconference, as a service for entertaining (video chat), educational (virtual classrooms) and communicating (through voice or sign language) purposes, is now held through Multipoint Control Units (software or hardware) that employ a centralized management for better quality of the sessions. In such a case, the traffic from the clients to the MCU is highly influenced by the parameters of the possible scenarios-modes of the MCU (codec used, number of participants, video bit rate, frame rate). Most of these factors (as will be commented upon later) change the statistical

[1] Although newer versions of the H.263 codec exist, namely, H.263+, H.264 they are not yet widely used and most videoconference clients do not support them.

characteristics of the generated traffic (an issue also studied in [4] and [20]).

Moreover, besides a few studies whose subject of research was videoconference traffic, all other studies (concerning vbr and MPEG video traffic modeling) use movies as the video source of their experiments (like Star Wars) that exhibit abrupt scene changes. However, the traffic pattern generated by differential coding algorithms (like those used by H.261 and H.263) depends strongly on the variation of the visual information. For videoconference, visual information does not contain abrupt scene changes, as videoconference coding algorithms were designed for a typical 'head and shoulders' content.

Due to the above context, the research reported in this paper undertook measurements of the IP traffic generated during videoconference 'talking heads' sessions (at 'switched presence'[2] mode) between four (4) commercial H.263-compliant clients that were using a different videoconference software package. At 'switched presence' mode, the MCU sends to all terminals the output from one participant, designated as 'currently active'. Thus, the videoconference traffic from the MCU to the terminals is not complex and not of particular interest (compared to 'continuous presence' where the MCU combines the signal from all terminals and sends back the output to all the participants). The experiments covered cases with both hardware and software MCU. The video source content was created realistically (a person speaking with mild movement and no abrupt scene changes). For the purpose of the statistical comparison of the different terminals' video traffic, the same produced content was used in all cases.

It has to be stressed that our traffic modeling approach, in this paper, focuses on queueing studies on the network performance. Thus, particular attention is paid on properties such as the long-term trends in the autocorrelation function and the tail[3] behavior of the frame size distribution (features not thoroughly examined in previous studies).

More analytically, the model proposed in this paper satisfies the following requirements (according to the recommendations towards a *good* traffic model that were proposed in [26]):

(a) *Realistic*: our model represents real-time encoded traffic sources as the traces were collected on-line during experiments with widely used commercial videoconference applications.

(b) *Reusable*: the term implies that the model must be as applicable as possible in any environment and must cover a wide range of experimental conditions. Our model is reusable as it covers a variety of experimental parameters: different videoconference applications, low and high motion head and shoulders content, different session parameters. Moreover, reusability demands that the coded traffic from the source must be as completely and as faithfully represented by the model as possible so that it can be applicable in any IP environment (LAN or WAN). Towards this direction two solutions can be directly applied: off-line encoding (as performed in [20]) or on-line encoding without bottlenecks (as in [26]). The former method does not provide realistic models (does not meet requirement (a)) while the latter demands that the experiments are conducted in an uncongested environment (like a backbone LAN environment). This will assure that no packet losses exist during the trace collection process and that the traffic model will always represent the best quality of the encoded video. The current study adopted the second method to meet both the (a) and (b) requirements. Taking into consideration the above, it is stressed that, in the current study, there was no point in investigating a WAN (or Internet-based) environment. It is evident that the proposed model is applicable in any IP environment as it represents source-faithful videoconference traffic encoded during UDP communication of IP terminals.

(c) *Parsimonious and computationally efficient*: we focus on the proper selection parameters of the simple and well established Markovian model DAR(1) and not on complex and compound models.In addition to the above, we believe that a *good* model has also to meet the following requirement:

(d) *Conservative (requirement not examined in previous studies)*: the model must be conservative as regards its application on performance evaluation in queueing studies. In detail, the resulting model should provide a conservative (but also closely accurate if possible) traffic characterization during queueing studies (i.e. more pronounced buffer occupancies, hence more probable overflows and longer queueing delays).

The rest of the paper is structured as follows: Section 2 discusses the videoconferencing platform employed for experimentation, describes the scenarios of the experiments and presents some basic statistical information of the measured data. Section 3 proposes methods for the modeling of the generated traffic for all cases and presents a full C-DAR(1) scheme for H.263 traffic modeling. Finally, Section 4 culminates with conclusions and pointers to further research.

2. Description of the videoconference experiments

The experiments of the present study were realized on two different platforms (see Fig. 1(a) and 1(b)). The two

[2] 'Continuous presence' mode has been extensively studied in [1] for H.261 video traffic. However, the focus of our study is the H.263 traffic generated by terminal clients and not by the MCU.

[3] As will be commented upon later, what matters in videoconference traffic modeling is the tail dominance of the model and not necessarily its fitting accuracy.

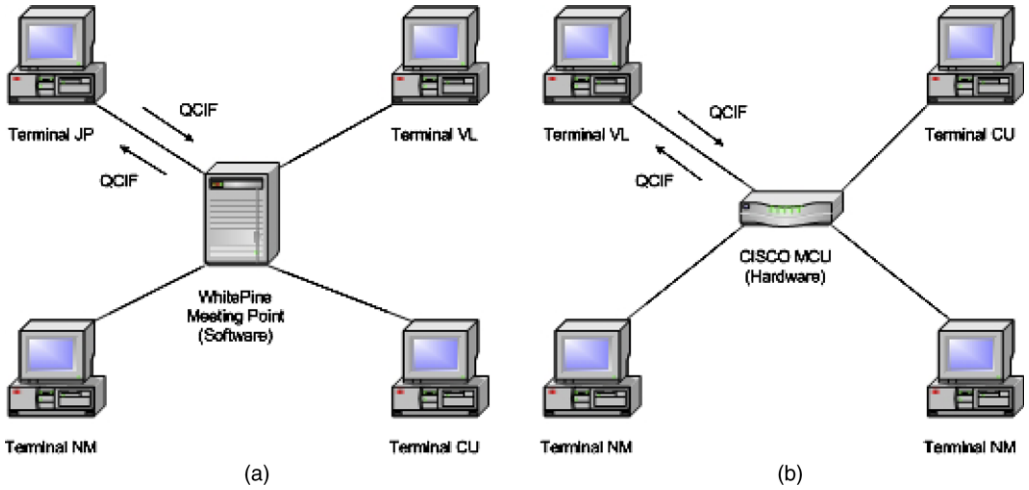

Fig. 1. Testbed topologies in an uncongested LAN environment. JP, JoinPhone Lite; VL, Video Link Pro; NM, NetMeeting; CU, CuSeeMe.

platforms consisted of personal computers running H.263-compliant videoconference software packages and an MCU, all networked over an uncongested IP-based LAN environment (100 Mbps). Four different videoconference software packages were used: MS NetMeeting 3.0 (NM), VideoLink Pro 3.0 (VL), CuSeeMe Pro 4.0 (CU) and JoinPhone Lite (JP) and two different MCUs: CISCO IP/VC 3510 unit (Hardware) and WhitePine Meeting Point Server (Software). All the experiments were held at the 'switched' presence mode where QCIF[4] H.263 videos are sent by all terminals to the MCU and a QCIF video is returned back (that of the 'currently active' user).

The current study examined four different factors which influence the traffic patterns generated by the terminals. These factors are presented along with the way they are tested:

- *H.263 implementation*: use of different videoconference software package for each terminal
- *Quality of the encoded video*: use of different target video bit rate in the MCU configuration
- *Target frame rate*: use of target frame rate in the MCU configuration—it is noted that a target frame rate was configured only for the CISCO MCU as Meeting Point did not pose any restriction on it. This is a basic reason of the use of both MCUs
- *Motion of the videoconference content*: use of two visual contents, a high-motion and a low-motion content.

The study focuses on how the above factors influence (or not) the first order statistics of the terminal-generated H.263 traffic. The answer, as supported by the consistent evidence from the experiments results, will be discussed below.

Under the needs of the above context, three experiments were designed, two with a software MCU and different session quality and one with a hardware MCU. All the software packages of the terminals were configured with the same video parameters for all the experiments (H.263—High Quality—QCIF). The terminals did not pose any restriction on the peak frame rate, except from JoinPhone Lite that was configured at a peak rate of 16 frames/s. A summary of the relevant quantities for each experiment is shown in Table 1. It is pointed that JoinPhone Lite could not join the session of the hardware MCU, due to the restriction on its peak frame rate. Thus, NM was used instead for experiment 3 with a different visual content (VC-L). 'VC-H' and 'VC-L' stand for video content with high motion and video content with low motion correspondingly. Both video contents are typical 'head and shoulders' videos with different motion. The two different video sources were used as the input of NM in experiment 3 to test the influence of the video content motion on the H.263 traffic pattern.

In each case, the IP packets exchanged between the terminals and the MCU were captured by traffic monitoring software (Ethereal). The collected data were further post-processed at the frame level by tracing a common packet timestamp. The produced sequences were used for further analysis.

It is important to note, here, that the analysis of previous studies at the GOP or MB level has been examined and found to provide only a typical smoothing in the sample data. We believe that the analysis of videoconference traffic at the frame level offers a realistic view of the traffic and is better for queueing studies.

Some first conclusions, as supported by the experiments' results (Table 1), arise concerning the influence of the four factors reported earlier. These are the following:

- There are some first clear indications of the statistical differences of the respective traffic patterns (although the same video settings and visual content have been used). It is already obvious that the four terminals utilize a different implementation of the H.263 video codec.

[4] We chose the QCIF format because this is the most commonly used format in commercial videoconference applications.

Table 1
Summary of relevant quantities for each experiment

Experiment	1				2				3			
MCU	WhitePine Meeting Point (Software)				WhitePine Meeting Point (Software)				CISCO MCU 3510 (Hardware)			
Software of terminal client	JP	NM	VL	CU	JP	NM	VL	CU	NM	NM	VL	CU
Video source	VC-H	VC-H	VC-H	VC-H	VC-H	VC-H	VC-H	VC-H	VC-H	VC-L	VC-H	VC-H
MCU frame rate (Frames/s)	–				–				15			
MCU video bit rate send/ received (Kbits/s)	300/300				100/100				300/300			
Parties	4				4				4			
Experiment duration (s)	3600				3600				3600			
Video frames	31,745	10,7972	41,260	48,884	31,750	94,654	38,096	17,437	54,302	54,242	38,215	45,768
Mean video bit rate (Kbits/s)	50	172	283	178	50	54	125	72	170	178	252	189
Mean frame rate (Frames/s)	9	30	11	14	9	26	11	5	15	15	11	13
Mean frame size (bytes)	713	715	3082	1640	716	256	1482	1859	1407	1480	2964	1855
Variance (bytes^2)	300,690	76,779	3,041,900	1,789,900	307,960	9765	1,419,300	2,842,600	135,450	76,310	2,822,100	2,949,600

VC-H, video content with high motion; VC-L, video content with low motion.

- The quality of the videoconference session (different MCU video bit rate used)—as clearly indicated in experiments 1 (300/300 Kbps) and 2 (100/100 Kbps)—influence the first order characteristics of all terminals besides JP (obviously due to the existence of a peak frame rate in its own configuration).
- The target frame rate factor is of no great importance for the traffic pattern (a small irregularity exists in the frame sizes histogram, as will be commented upon later). Most terminals are not influenced by the MCU target frame rate except from the terminal NM. In detail, NM tends to send frames at a higher rate (30 frames/s) when no target frame is set (experiments 1 and 2), while it sends at a lower frame rate (15 frames/s) in the case of experiment 3.
- The motion of the video content seems to influence the variance of the traffic pattern, a fact that implies a larger periodicity (lower complexity) in the traffic pattern (as remarked in experiment 3 by the comparison of the variance of NM with VC-H and NM with VC-L). This leads to the conclusion that the variance is a measure of the amount of motion of the videoconference content.

Generally, it is noted that the terminal VL sends video at a higher bit rate than the terminals CU and NM while the slowest of all is the terminal JP (apparently because of the frame rate restriction in its own configuration). Regarding frame sizes, NM[5] and JP produce smaller frames than VL and CU. It may also be observed that the values of the bit rate achieved are in all cases much lower than the respective maximum specifications of the MCU settings, reflecting the fact that the content of the videoconference did not exhibit dramatic scene changes, frequent zooms or other such effects. The next section will analyze the H.263 traffic of each terminal separately, proposing a corresponding traffic model and commenting more thoroughly upon the influence of the above factors.

3. Analysis of the video data sequences

The analysis of the H.263 traffic from all terminals to the MCU, for both experiments, confirms the general body of knowledge that literature has formed concerning videoconference traffic. In brief, the sequence of the frame sizes from a terminal can be represented as a stationary stochastic process, with an autocorrelation function quickly decaying to zero and a marginal frame-size distribution of approximately Gamma form. All frame-size distributions are Gamma-like (with a heavier tail[6]) and very asymmetrical (this can be seen in other studies of H.263 traffic too [4,20]).

[5] From now on, we will refer to the terminals JP, VL, CU, NM as JP, VL, CU and NM correspondingly.

[6] Tail behavior is a matter of great importance that affects queueing and will be examined thoroughly during analysis.

These general characteristics remain invariant for all the experiments.

In checking for stationarity, each frame sequence corresponding to a terminal was split in a moderate number of windows (ten) and then the empirical density function for the frame size was calculated from the sample in each window. These windows were found to be very much alike, property suggesting that the sequence is stationary. This is in accordance with the study in [1] where stationarity was found to apply for H.261 traffic. Thus, there is no point in further analyzing towards this point.

3.1. Autocorrelation function analysis

As can be seen in the graphs of the ACF fitted models (see Fig. 2(a), (c), (e), (g), (i) and (j)), the ACF of H.263 traffic seems to decay quickly (almost exponentially). The strong correlations in the ACFs of JP and NM (Fig. 2(a), (g), (i) and (j)) (implying periodicities in the traffic pattern) are attributed to the similarities (temporal redundancy) that exist between sequential video frames. The comparison of the experimental results showed that the ACF of H.263 traffic is not strongly influenced by the parameters of

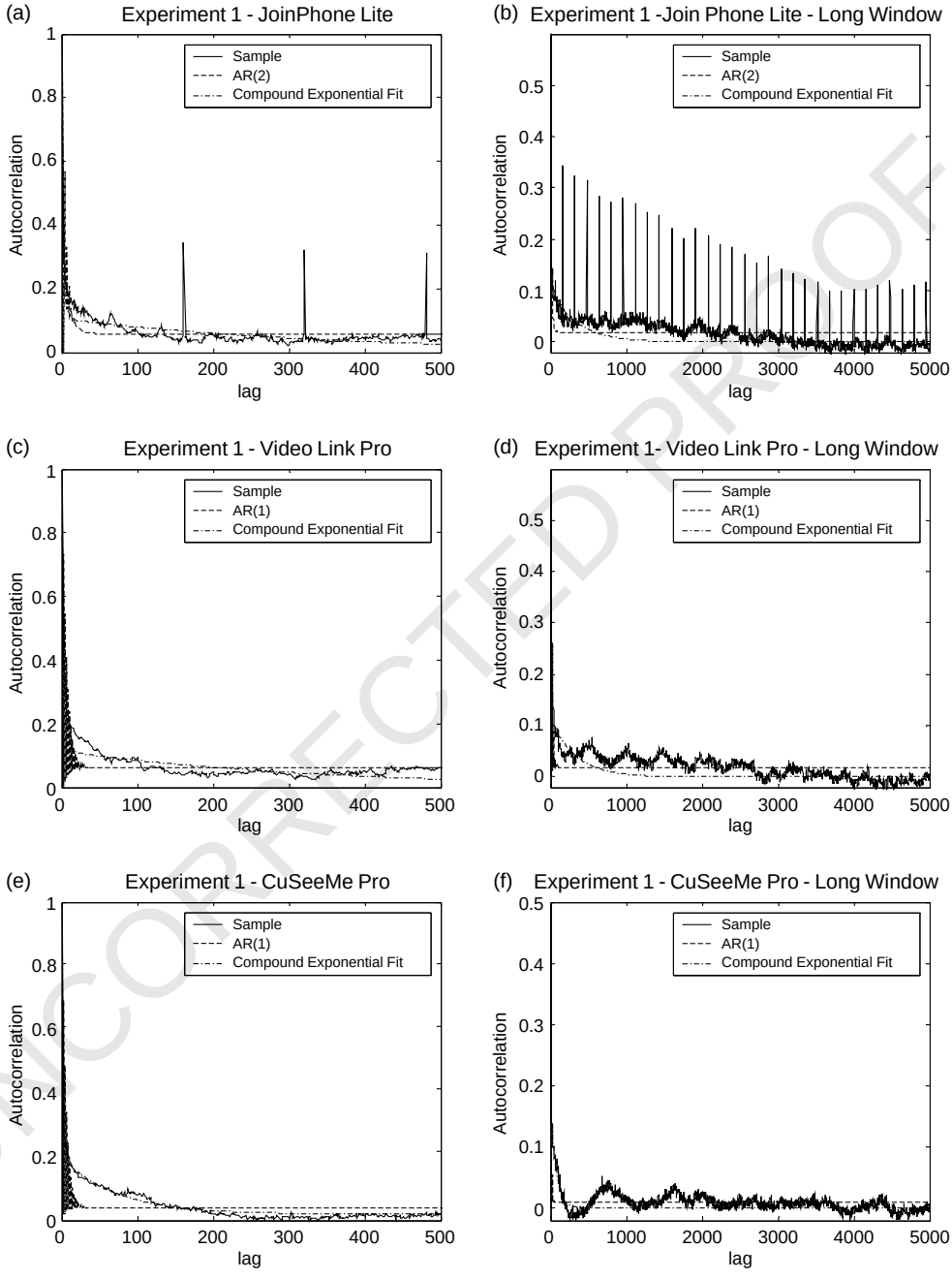

Fig. 2. Autocorrelation Graphs and fitted models for H.263 traffic from terminals.

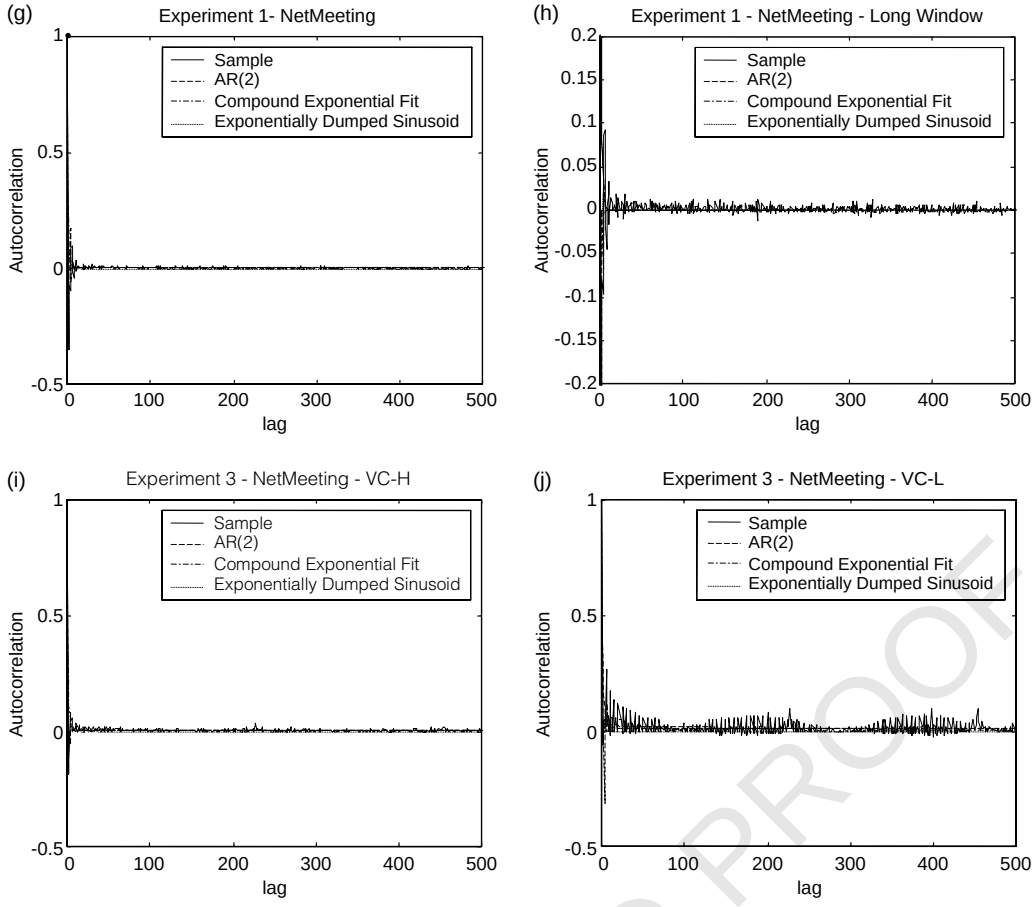

Fig. 2 (*continued*)

the videoconference session (quality and frame rate). Nevertheless, the ACF is different for each terminal, a fact obviously caused by the different implementations of the H.263 codec.

To be more specific, the ACFs of VL and CU (Fig. 2(c) and (e)) have an almost similar behavior, a fact that indicates the statistical resemblance of the two traffic patterns (implying similarities in the implementation of the H.263 codec of the two videoconference software packages). A strong periodicity every 160 lags can be seen in the ACF of JP (Fig. 2(a)), maybe suggesting that during the session, JP is periodically sending Intra frames at regular intervals. Even stronger correlations appear in the ACF of NM (Fig. 2(g), (i) and (j)).

The low-motion video content, 'VC-L', used in experiment 3 for NM, caused a larger periodicity in the ACF (see Fig. 2(j) compared to Fig. 2(i)). The results of the ACF analysis (graphs and fitted models) will be presented for each software terminal in experiment 1, for NM (VC-H and VC-L) in experiment 3 and numerical values of the fitted models will be given for all experiments.

To find the most accurate fitting model for the ACF of H.263 traffic, three different methods, reported in literature were used. The first two were proposed for modeling H.261 terminals traffic in multipoint videoconference at 'continu-continuous presence' [1]. The third one is an AR-based approach proposed in [12] that estimates the parameters and eigenmodes of AR models of arbitrary order. In our study the particular method was used to estimate the parameters of the correlation coefficients of the AR(1) and AR(2) models[7]. More analytically, the methods used are the following:

1. A weighted sum of two geometric terms [1]

$$\rho_k = w\lambda_1^k + (1-w)\lambda_2^k, \quad \text{with } |\lambda_2| < |\lambda_1| < 1 \tag{1}$$

2. A geometrically dumped sinusoid [25] of the form:

$$\rho_k = \frac{\lambda^k \cos(\theta_k + \psi)}{\cos\psi} \tag{2}$$

3. AR(1) and AR(2) models:

$$\mathrm{AR}(1) : X_n = w + \alpha_1 X_{n-1} + C \tag{3}$$

$$AR(2) : x_n = w + \alpha_1 X_{n-1} + \alpha_2 X_{n-2} + C \tag{4}$$

[7] Although literature reports that AR(2) [13] or even of higher order AR(p) models [24] produce a better match than AR(1) models, AR(1) seems to perform well for H.263 traffic (as will be commented upon later).

Table 2
Model parameters fitted to sample ACF

Exp	1												
	Compound exponential fit			Dumped sinusoid fit			AR(1)			AR(2)			
	$\rho_\kappa = w\lambda_1^\kappa + (1-w)\lambda_2^\kappa$			$\rho_\kappa = \lambda^\kappa \cos + (\theta_\kappa - \psi)/\cos\psi$			$X_n = w + \alpha_1 X_{n-1} + C$			$X_n = w + \alpha_1 X_{n-1} + \alpha_2 X_{n-2} + C$			
	w	λ_1	λ_2	λ	θ	ψ	w	α_1	C	w	α_1	α_2	C
JP	0.1058	0.9972	0.6803	0.1355	6.2832	4.7124	0.0297	0.4854	0.00091641	0.0177	0.4853	0.2001	0.0007129
NM	0.0008	0.9999	0.4288	0.2972	1.957	−1.329	0.0002154	−0.2809	0.00002492	0.0002336	−0.0974	−0.0839	0.000018642
VL	0.1144	0.9970	0.759	0.2024	−6.283	1.5708	0.0025	0.8695	0.000041826	0.0004708	1.2107	−0.2372	0.000012335
CU	0.1822	0.9861	0.6143	0.1319	6.2832	4.7124	0.0056	0.6814	0.00041838	0.0001146	1.1021	−0.1286	0.000018573
Exp	2												
JP	0.0992	0.9972	0.6801	–	–	–	0.0293	0.4619	0.001	0.019	0.4431	0.2018	0.00085667
NM	0.0013	0.9996	0.4584	0.2295	1.9973	−1.383	0.0018	−0.2193	0.000085027	0.0013	0.2564	0.0313	0.000051467
VL	0.0811	0.9985	0.8044	0.3881	6.2728	1.8212	0.0155	0.7295	0.00014596	0.0031	1.1671	−0.2255	0.000015599
CU	0.793	0.9985	0.7283	–	–	–	0.0401	0.7177	0.00022243	0.0067	1.1108	−0.1606	0.000034146
Exp	3												
VL	0.0977	0.9972	0.7435	–	–	–	0.0174	0.675	0.00015733	0.0025	1.2185	−0.2685	0.00068922
CU	0.8414	0.9782	0.644	0.7457	18.85	4.7134	0.0018	0.6359	0.00031755		0.9784	−0.0463	0.000044459
NM (VCH)	0.0222	0.9963	0.525	0.0307	3.1386	−1.571	0.013	−0.153	0.00074	0.014	−0.3218	0.0578	0.000018346
NM (VCL)	0.0052	0.9975	0.4712	0.3796	1.634	−1.216	0.0037	−0.1564	0.00010112	0.0044	−0.089	−0.1489	0.000026151

Methods (1) and (2) were tested with a least squares fit to the autocorrelation samples for the first 500 lags. Method 3 returns least squares estimates of the intercept vector w, of the coefficient matrices α_1, α_2 and of the noise covariance matrix C. All models were compared against the samples over a wider range of lags (up to 5000) to verify that they are capable of capturing the long-term trends of the ACF decay. Numerical values for the results appear in Table 2, while the graphs of the fitted models are compared to the sample ACFs in Fig. 2. The most dominant model for all cases is the Compound Exponential Fit as it is able of capturing the long-term trends of the ACF better than the other models (see Fig. 2(b), (d), (f) and (h)). The dumped sinusoid (of similar behavior as in [1]) did not fit well (decayed much faster than the sample ACF) and thus is not depicted. Only in case of NM, where very strong correlations exist, it produced a satisfying fit (see Fig. 2(g), (i) and (j)). AR(1) performed satisfactorily for VL and CU where AR(2) failed to fit (see Fig. 2(c) and (e)). On the contrary, AR(2) was better in cases of JP and and NM where AR(1) failed (see Fig. 2(a) and (g)). It is insighted that AR(1) performs well in traffic patterns with no strong correlations (such as ACFs of VL and CU) while AR(2) is better for cases where periodicities exist (ACFs of JP and NM).

Taking into account that the long-term decay rate is the most important factor for queueing, it is evident that a proper model for fitting the autocorrelation function of H.263 traffic is the Compound Exponential Fit. In fact, what matters is the autocorrelation coefficient λ_1 in (1) as it tends to capture the long-term behavior of the ACF. The retention of this model is further verified by previous studies [1,13] for videoconference traffic where values of λ_1 were found to be near 0.98 (see Table 2 for numerical values of λ_1). This being the case, a further study towards new or more complex models is of no point.

3.2. Probability distribution function analysis

Now, we may proceed to the analysis of the PDF of the traffic patterns' frame sizes which is one of the main points of the current study. In actuality, all the density distributions seem to fit a Gamma-like shape with a heavy tail and asymmetry. This is less obvious in the case of NM whose PDF is bell-shaped (see Fig. 5(d), (e), (f)) (fact confirmed by a previous study of H.261 traffic of the terminal NM [1]). On the contrary, the PDFs of JP, VL and CU are strongly asymmetrical (see for example Figs. 3(g), 6(g) and 7(h)) in all cases. This irregularity makes it difficult to find a good distribution that fits reasonably well. Several distributions have been proposed for fitting the PDF of videoconference traffic, other simple (e.g. Gamma, Log-normal, Weibull) and other more complex (e.g. compound normal distribution). However, the one established and mostly used in video traffic modeling is the Gamma density function. This being the case, in this study, we focused on the proper selection of the parameters of the Gamma density and not on

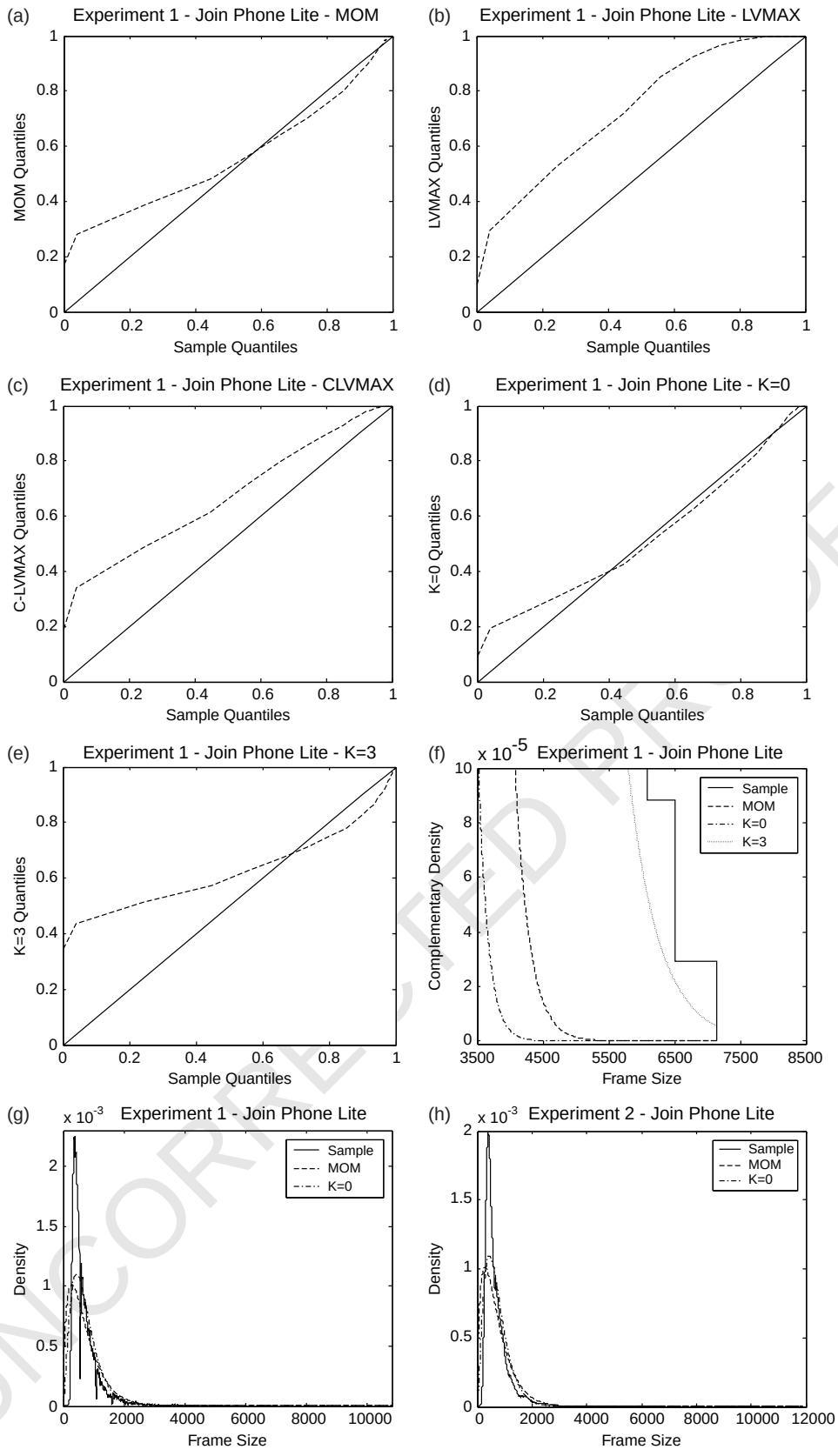

Fig. 3. Frame size histograms-Gamma models, *Q–Q* plots and complementary probability functions for terminal JP in experiment 1.

finding new complex, heuristic solutions that would probably not meet the requirements (b) and (c) reported in Section 1.

On the basis of using a single distribution to fit the empirical data, we have to note that the complex nature of the sample PDF can never be perfectly 'captured' by a distribution generating frame sizes according to a declared mean and standard deviation, and therefore, none of the fitting attempts (including the Gamma density), as good as they might be, can achieve perfect accuracy. However, there is a basic requirement that the model should meet in order to be suitable for further analysis (with respect to queueing). The model must be tail dominant (feature included in the requirement (d)): that means that the probabilities values of the model around the PDF tail must be lager or approximately equal to the corresponding values of the sample. The distribution tail, by containing the probabilities of events corresponding to large frames, thus high bit rates, is a critical aspect to capture in a queueing model. Neglecting, it may cause wrong calculations in buffer overflow estimations.

On the above basis, the Gamma density function will be used to fit the empirical PDFs.

$$f(x) = \frac{1}{\Gamma(p)}\frac{1}{\mu}\left(\frac{x}{\mu}\right)^{p-1} e^{-(x/\mu)}, \mu, p > 0, x \geq 0$$

where

$$\Gamma(p) = \int_0^\infty u^{p-1}\mathrm{e}^{-u}\mathrm{d}u \tag{5}$$

To calculate the p and μ parameters of the Gamma density, three previously applied methods and a class of new methods were evaluated. The older ones were used for modeling H.261 traffic from NM terminals to the MCU in [1] while the new methods are based on a class of methods of moments estimators for the Gamma density, presented recently in [22]. More explicitly, the first three methods are the following:

1. MOM (Methods of moments). When the mean, m, and the variance, v, of the data sample are known, the method of moments produces estimates for the shape and scale parameters of the Gamma distribution:

$$p = \frac{m^2}{v} \text{ and } \mu = \frac{v}{m}$$

2. LVMAX. The LVMAX method relates the histogram's peak to the location at which the Gamma density achieves its maximum and to the value of this maximum. The values of the shape and scale parameters are derived from:

$$p = 2\pi x^{*2} f^{*2} + 1 \text{ and } \mu = \frac{1}{2\pi x^* f^{*2}}$$

where f^* is the unique maximum of the histogram density at x^*.

3. C-LVMAX. The third method is an application of the LVMAX method to the self-convolution of the histogram. In this method:

$$p = \frac{2\pi x^{*2} f^{*2} + 1}{2} \text{ and } \mu = \frac{1}{2\pi x^* f^{*2}}$$

As will be commented upon later, the above three methods were tried and, except the conventional MOM method, were not tail dominant in most cases.

4. $K=k$. The class of methods of moments estimators studied in [22] is a new body of knowledge in statistical science and (to the best knowledge of these authors) has never been tested for videoconference traffic modeling. The members of this family are very easy to compute, relative to the maximum likelihood estimation or its commonly used approximation. More specifically, this method is a class of moment estimators (a vector $\boldsymbol{\theta}_k$ of values for p and μ):

$$\boldsymbol{\theta}_k = (p_k, \mu_k)^T \text{ with } \mu_k = \frac{m}{p_k},\ k \geq 0$$

If $\mathbf{x}=(x_1, x_2,\ldots,x_n\}$ is the vector of the data sample (frame sizes) and the vector $\boldsymbol{x}_k = \{x_1^k, x_2^k, \ldots, x_n^k\}$ then the values for the p and μ parameters of the Gamma function are easily calculated as follows:

$$p_k = \frac{m m_k}{k^{-1} S(\boldsymbol{x}_k, \boldsymbol{x})}, k > 0$$

$$p_k = \frac{m}{S(\ln \boldsymbol{x}, \boldsymbol{x})}, k = 0$$

where m is the mean of $\mathbf{x}$, m_k the mean of $\mathbf{x}_k$ and $S(\mathbf{a},\mathbf{b})$ the covariance of the vectors $\mathbf{a}$ and $\mathbf{b}$. The flexibility of this method is evident as for various values of k ($k \geq 0$) new values for the shape and scale parameters are computed and as a result a different fitting method is tested. From now on, in the current study, this method will be referred to as $K=$ 'value of k' (for example $K=0$, 2, 3). As will be proved later, this method has been tried as an unconventional fitting method (although sufficiently simple) due to its ability to capture conservatively (asymptotically tight though) the tail region of the PDF (meeting in this way the requirement of tail dominance (d)).

After extensive testing, we concluded that among the class of the fourth method only the $K=0$ and 3 models are suitable (with respect to queueing behavior) for H.263 traffic. Especially, the $K=3$ model has the advantage of capturing conservatively the PDF tail, a fact that makes it suitable for further queueing analysis. Given these conclusions, modeling analysis and evaluation will be presented for the following five methods: MOM, LVMAX, C-LVMAX, $K=0$ and 3. The numerical results (p and μ values) from the application of the above parameters-matching methods in the data appear in Table 3.

The modeling evaluation of the above methods has been performed from the point of queueing. As a consequence, we thoroughly examined fits of cumulative distributions

Table 3
Gamma parameters for the various fitting methods applied to the terminals' data

			LVMAX		C-LVMAX		$K=0$		$K=3$	
	p	μ	p	μ	p	μ	p	μ	p	
Exp	1									
JP	1.69	421.51	5.56	83.09	2.36	223.98	2.67	267.29	0.74	961.15
NM	6.66	107.33	13.71	66.19	7.94	102.78	5.44	131.52	8.46	84.58
VL	3.12	987	7.69	250.21	4.32	623.82	4.02	765.75	2.03	1521.8
CU	1.5	1091.4	2.53	444.62	1.5	970.59	1.98	828.29	1.04	1580.5
Exp	2									
JP	1.66	430.39	6.24	76.47	2.44	214.69	2.67	267.87	0.66	1082.5
NM	6.73	38.1	21.74	13.41	12.96	21.43	7.51	34.12	2.43	105.59
VL	1.55	958.02	4.79	182.78	2.8	473.35	2.19	677.14	1.04	1418.2
CU	1.22	1529.1	2.24	500.3	1.05	1523.3	1.53	1216.3	1.01	1846.9
Exp	3									
NM (VC-H)	14.62	96.27	24.34	66.5	15.23	94.36	12.87	109.37	16.92	83.15
NM (VC-L)	28.7	51.56	61.41	25.94	40.34	38.41	25.4	58.27	32.52	45.51
VL	3.11	952.27	8.73	219.92	4.47	606.52	4.04	734.07	2.02	1468.1
CU	1.17	1589.9	3.14	394.37	1.27	1174.2	1.68	1107.5	0.84	2213.7

and dominance in the tail region. This was done as follows: the sample and the model quantiles were plotted to test fitting accuracy (Cumulative Q–Q plot). The sample quantiles derive from the PDF (cumulative distribution) of the sample and the model quantiles from the incomplete Gamma function $f_{\text{inc}}(x/\mu,p)$ of the corresponding model where:

$$f_{\text{inc}}(x,p) = \frac{1}{\Gamma(p)} \int_0^x \mathrm{e}^{-1} t^{p-1} \mathrm{d}t \tag{6}$$

and $\Gamma(p)$ derives from (5).

The Q–Q plots of the above method refer to cumulative distributions (probabilities of not exceeding a threshold). Thus, the tail behavior for the fit is indicated by the neighborhood of quantiles around 1. If the model's quantiles are lower than the sample quantiles in that neighborhood, the model is considered to be conservative (with respect to queueing). For more detail around that neighborhood, the complementary PDF is plotted together with the complementary Gamma function in the large frames region (tail). This method gives valuable indications about the tail behavior of each model (tendency of the model to move to 'high bandwidth' states) and a measure of their conservativeness concerning queueing.

In the following paragraphs, PDF modeling will be performed applying the above methods. Modeling results, commented for each case separately, lead to conclusions about the proposed models.

3.2.1. PDF analysis of terminal JoinPhone lite

The probability distribution functions of the traffic generated by JP were found to be strongly asymmetrical, see Fig. 3(g) and (h). Both the traffic patterns of JP in experiments 1 and 2 were statistically identical reflecting the fact that there was no influence of the videoconference session parameters on the generated traffic pattern.

The Q–Q plots of experiments 1 and 2 (results are depicted only for experiment 1) showed that the MOM and $K=0$ models performed better with respect to the requirement of tail dominance (see Fig. 3(a) and (d)) than the LVMAX and C-LVMAX models (Fig. 3(b) and (c)). More analytically, the MOM and $K=0$ methods did not manage to follow closely the histogram in all quantiles (especially in the first ones and more notable in the case of MOM). However, this phenomenon is not critical with respect to queueing as what is important is the conservativeness of the model at the higher rate states (large frame sizes). The model $K=3$, although being conservative in the large frames region (tail), declines considerably in the small frames region (Fig. 3(e)). The complementary density plot of Fig. 3(f) indicates the tail behavior of the MOM, $K=0$ and 3 model. Finally, the PDFs and the Gamma models for MOM and $K=0$ are depicted in Fig. 3(g) and (h) for experiments 1 and 2 correspondingly (as reported previously, terminal JP did not join the videoconference session of the experiment 3).

3.2.2. PDF analysis of terminal NetMeeting

The frame size histograms of NM were found to be symmetrical enough compared to the other terminals. In experiment 1, the absence of a target frame rate caused a greater than usual irregularity in the small frames region as shown in Fig. 4(h) and (i). In a lower video bit rate session (experiment 2), the frame size histogram consisted mostly of the small frames contribution and as a consequence, the PDF was more narrow and tall (see Fig. 5(d)). More explicitly, in experiment 1, the models MOM, C-LVMAX, $K=0$ and 3 were found to be the most dominant (see Fig. 4(a)–(e)). The MOM, C-LVMAX and $K=0$ models

were the most conservative whereas the $K=3$ model fitted accurately the PDF tail as shown by the Complementary density plot in Fig. 4(f) and (g). The same analysis in experiment 2 for NM showed that C-LVMAX performed better than $K=0$ while $K=3$ did not perform well (see Fig. 5(a)–(c)). The analysis of the experiment 3 led to similar conclusions with the experiment 1. The MOM, C-LVMAX and $K=3$ models were found to be the most dominant for both cases of visual content used (VC-H and VC-L). The PDF with the most dominant models are plotted for experiments 2 and 3 in Fig. 5(d)–(f).

It is evident by the above results that the MCU session parameters (frame rate, video bit rate) and the motion of the visual content, although they change the shape of the PDF, do not influence dramatically the performance of the theoretical models.

3.2.3. PDF analysis of terminal video link pro

The analysis of the frame-size histograms for all the VL experiments reflected clearly the non-influence of the session parameters (frame rate, video quality). In all cases, the PDFs of VL exhibit a similar asymmetrical bell-like

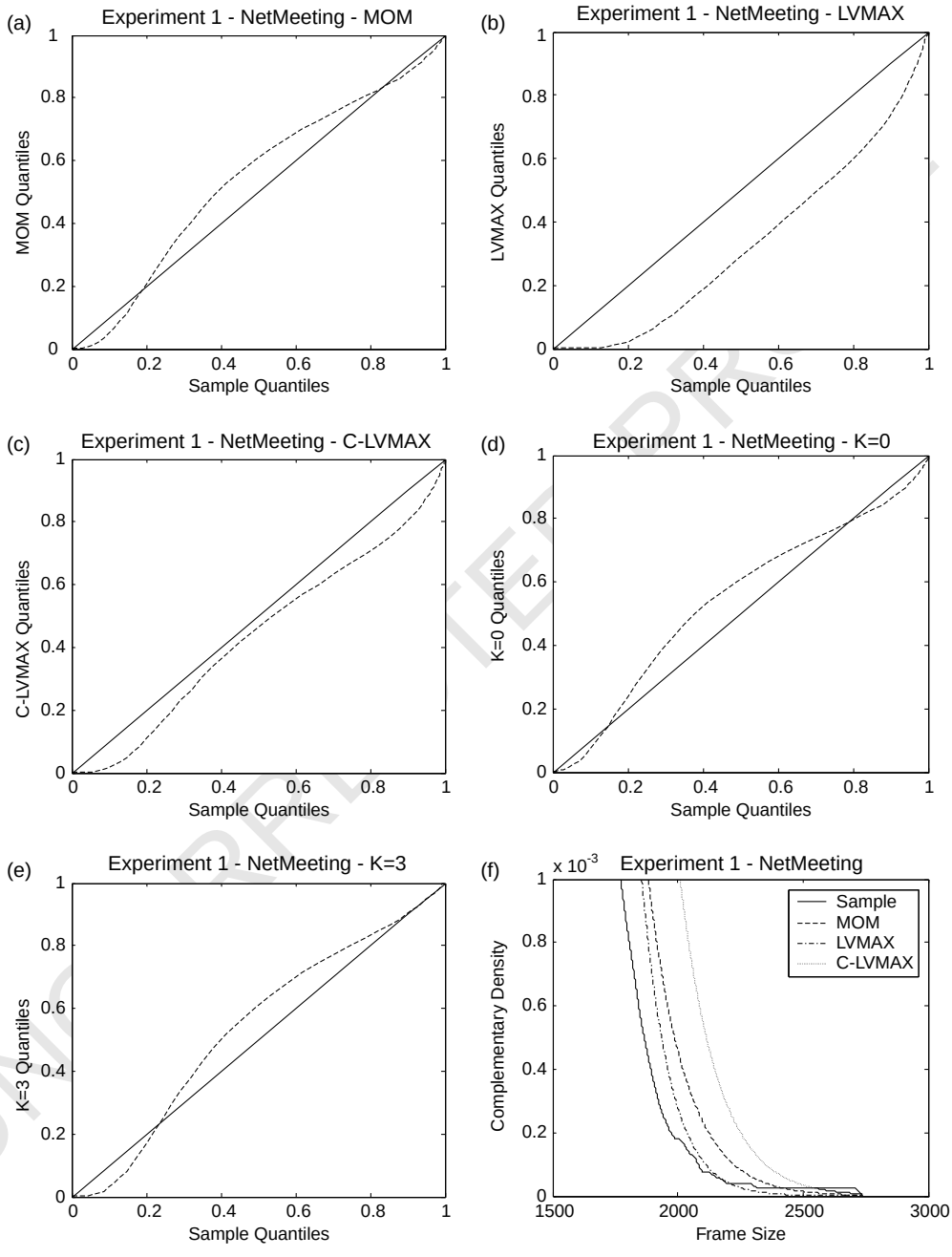

Fig. 4. Frame size histograms-Gamma models, *Q–Q* plots and complementary probability functions for terminal NM (experiment 1).

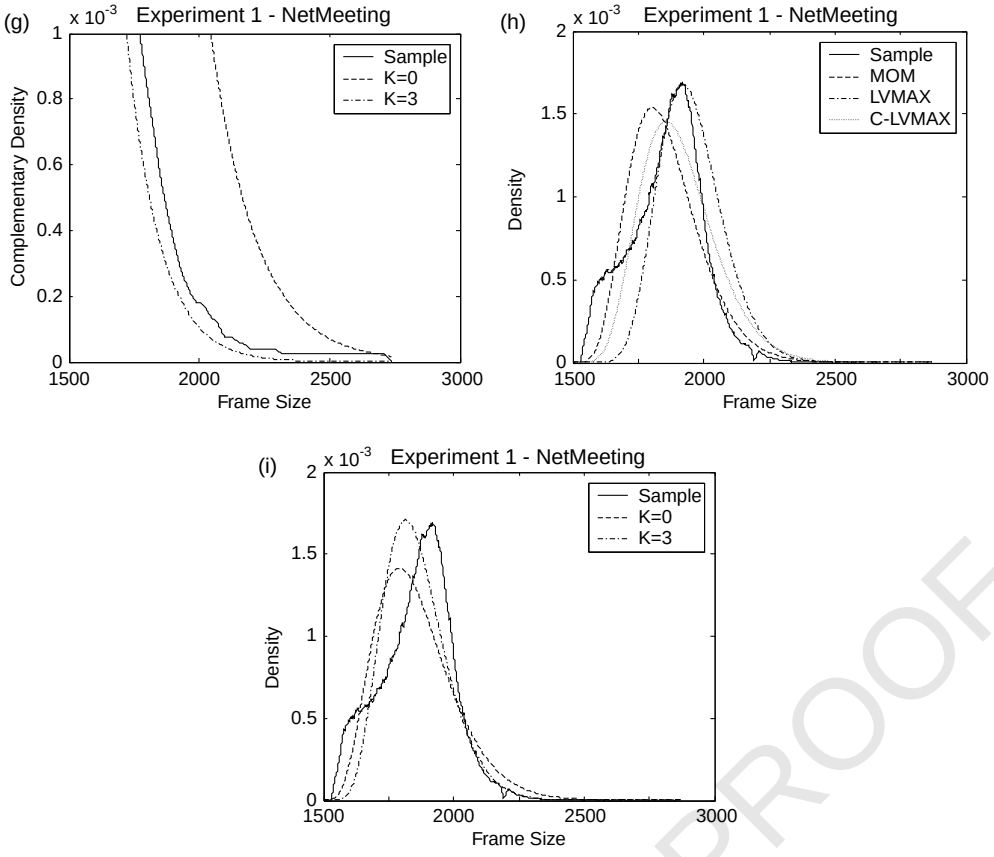

Fig. 4 (*continued*)

shape (see Fig. 6(g), (i) and (j)). Thus, the modeling results will be presented for the first experiment and PDFs will be given only for experiments 2 and 3 with the fit of the most dominant models. *Q–q* plots in Fig. 6(a)–(e) prove that the most conservative and tail dominant models are again the MOM, $K=0$ and 3 (see Fig. 6(h) for the fitted PDF plot). The LVMAX and C-LVMAX was, as in the case of JoinPhone Lite, non-conservative. Although the MOM and $K=0$ models seem to perform better, $K=3$ model is more tail dominant as depicted in Fig. 6(e) and (f). Fig. 6(g), (i) and (j) reflect the statistical resemblance of the traffic patterns generated by VL in all the experiments.

3.2.4. PDF analysis of terminal CuSeeMe Pro

The similar analysis for CU proved that the traffic patterns of the terminals VL and CU have statistical similarities. The modeling results are the same for both facts implying that a similar implementation of H.263 was applied in their software applications. The conclusions for the H.263 traffic of CU are the same for all experiments and thus full results will be presented again for the experiment 1. The Fig. 7(a)–(f) reflect the fact that MOM, $K=0$ and 3 models are the most dominant. Finally, the Fig. 7(g)–(j) depict the PDF plots with the most dominant models.

3.3. Queueing analysis via the C-DAR(1) model and the fluid-flow method

The C-DAR(1) model that was proposed and used analytically in [23] can be directly applied for full modeling and analytic treatment of H.263 traffic in multipoint videoconference sessions over IP networks. This model is defined as a continuous-time discrete-state Markov chain with a transition rate matrix Q of the form:

$$Q = f(P - I) \tag{7}$$

where

$f = \frac{\ln \rho}{\rho - 1} T$, $P = \rho \mathrm{I} + (1-\rho)A$ from DAR(1) [13], T is the frame rate of the H.263 traffic, I is the identity matrix, ρ is the autocorrelation decay rate and A is a rank-one stochastic matrix with all rows equal to the probabilities resulting from the negative binomial density of the form:

$y = f(x/r, P) = \binom{r+x-1}{x} P^x (1-P)^x$, $x = 0, 1, \ldots, r > 0$, $0 < P < 1$ corresponding to the Gamma fit for the frame size distribution. The parameters r and P of the negative binomial density are calculated by the parameters of the correspondent Gamma density with p and μ parameters as follows:

$$r = \frac{p\mu}{\mu - 1} \text{ and } P = \frac{1}{\mu}.$$

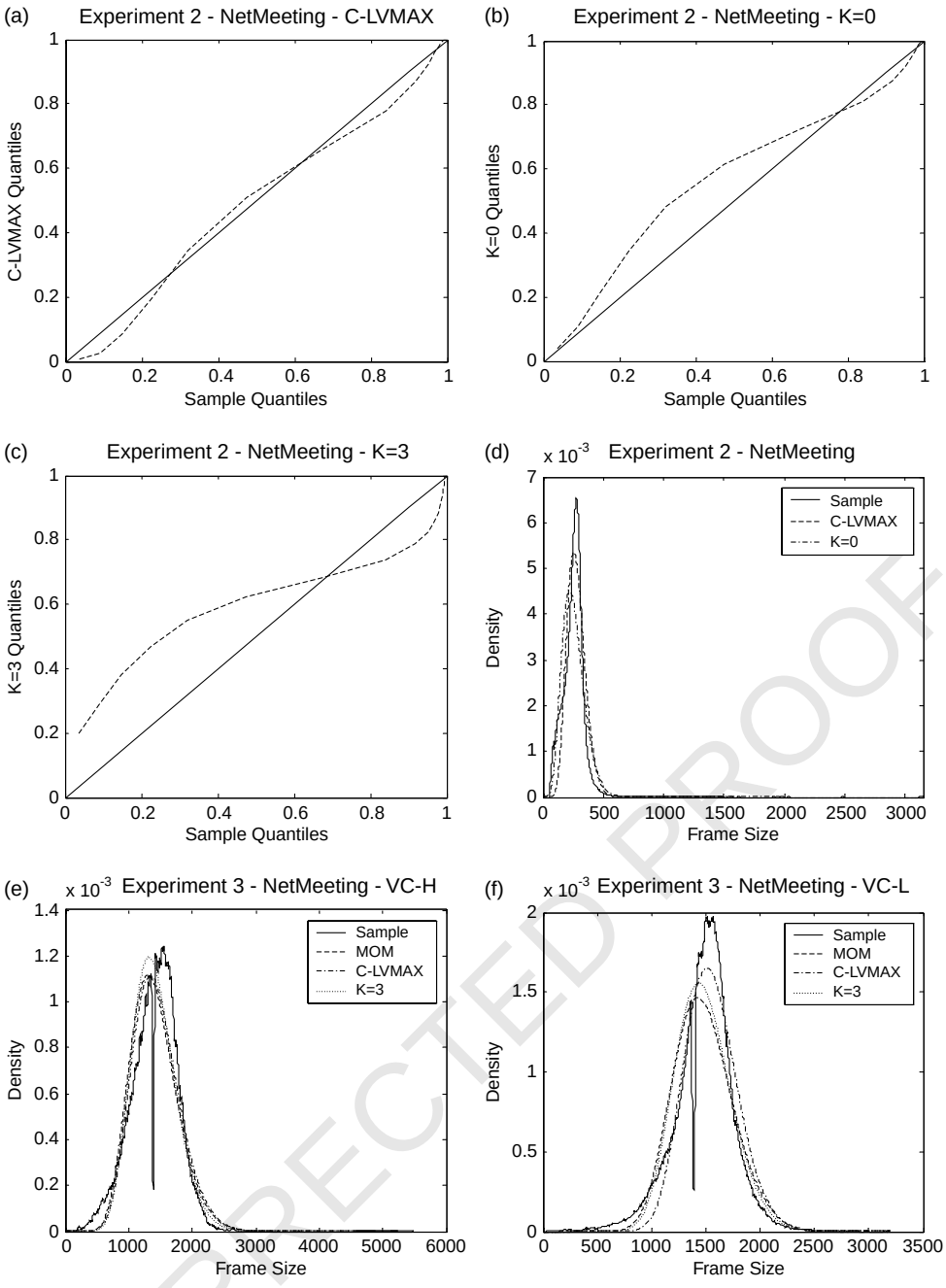

Fig. 5. Frame size histograms-Gamma models, Q–Q plots and complementary probability functions for terminal NM (experiments 2 and 3).

The value of the autocorrelation decay rate ρ should be chosen equal to the parameter λ_1 of the model used to fit the ACF (1) (see Table 2) and the elements for the rows of A should be determined through the Gamma fit produced by the PDF models.

Following the approach in [23], the C-DAR(1) model—as a continuous-time Markov chain model—is suitable for theoretical analysis using the fluid flow method [27–29]. This method is analyzed as follows: consider a single server queueing system fed by videoconference traffic $r(t) \geq 0$ as a Markov modulated rate process according to the C-DAR(1) model with a finite number of N states and transition rate matrix Q (from the C-DAR(1) model (7)). More explicitly, in each state $i = 1,\ldots,N$, we correspond a video rate r_i. If $\boldsymbol{\pi}$ is the corresponding steady state probability vector, then the mean input rate $\bar{r}$ is calculated as follows:

$\bar{r} = \sum_{i=1}^{N} \pi_i r_i$. Let $R = \mathrm{diag}\{r_1,\ldots,r_N\}$ and C the constant server capacity. When $r(t) > C$, the input traffic cannot be served entirely and its excess part is stored into a buffer in order to be served later. Let $\{X(t), t \geq 0\}$ the stochastic process that represents the buffer occupancy. It is noted that the traffic intensity of the system is equal to $\bar{r}/C$.

Define the steady state PDF $F_i(x)$ as the joint probability that the buffer occupancy is less than or equal to x, when in the i state of the source model. Let: $\mathbf{F}(x)=[F_1(x), F_2(x),\ldots,F_N(x)]^T$.

Then from [27–29] we have:

$$\frac{d\mathbf{F}(x)}{\mathrm{d}x}D = \mathbf{F}(x)Q \tag{8}$$

where $D=R\text{-}CI$.

Given the infinite buffer assumption, we determine a buffer threshold B and define the buffer overflow probability as follows:

$$\text{Poverflow} = 1 - \mathbf{F}(B)\mathbf{1} \tag{9}$$

where $1=(1,\ldots,1)^T$. From (8) and the boundary conditions for the infinite buffer size approach in [27–29], we can determine the vector $\mathbf{F}$. In detail, the following relation holds:

$$\mathbf{F}(x) = \sum_{i=1}^{N} \alpha_i e^{z_i x}\phi_i \tag{10}$$

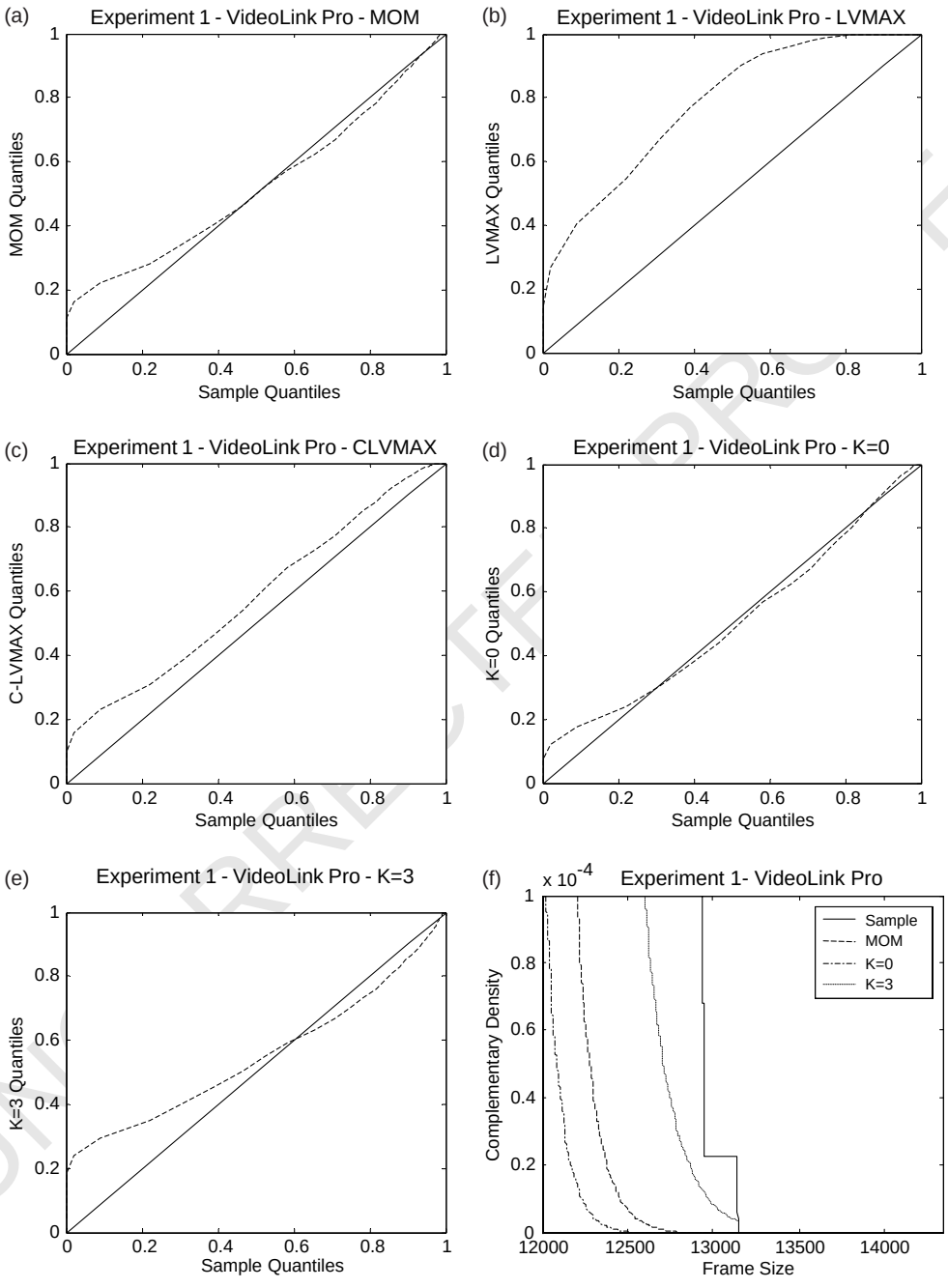

Fig. 6. Frame size histograms-Gamma models, Q–Q plots and complementary probability functions for terminal VL.

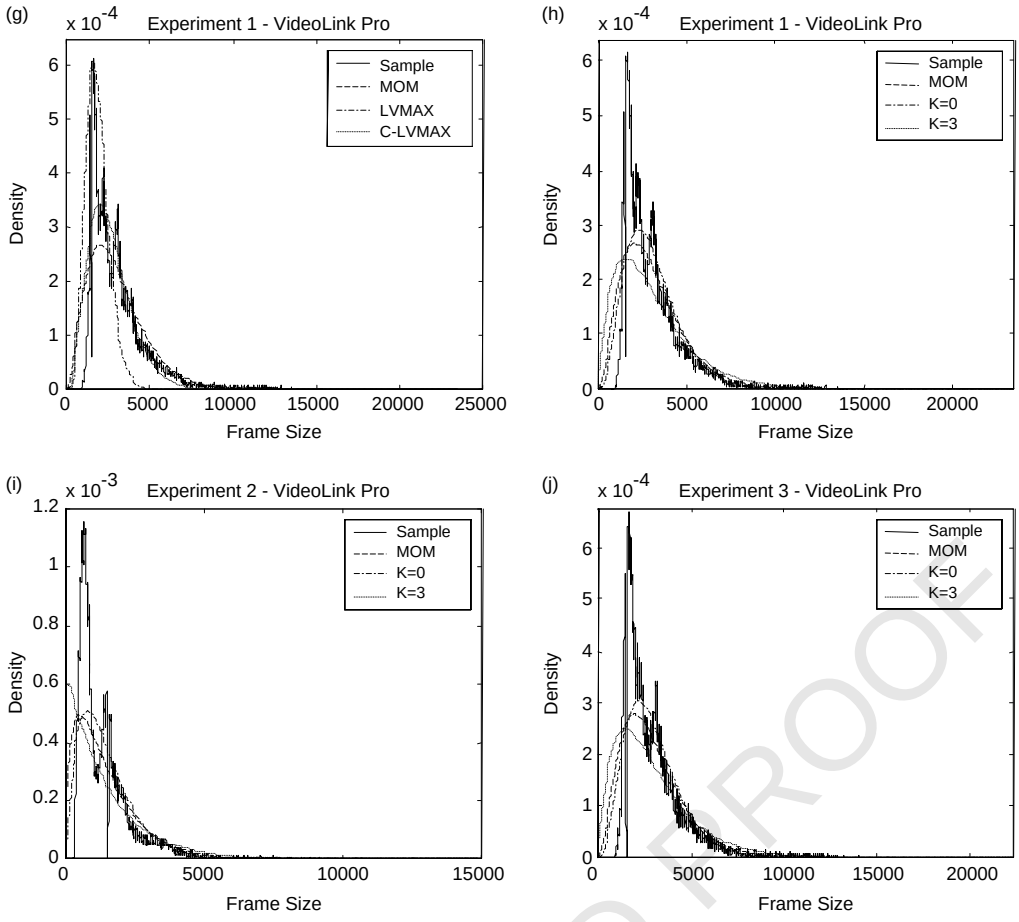

Fig. 6 (*continued*)

where the coefficients a_i must be calculated from the boundary conditions and z and ϕ are correspondingly, the eigenvalue and the left eigenvector of the matrix QD^{-1}. Given the infinite buffer assumption, the solution of (10) is given as follows:

$$\mathbf{F}(x) = \pi + \sum_{i \in S_o} a_i e^{z_i x} \phi_i \tag{11}$$

where

$$S_o \triangleq \{j | r_j > C\},\ z_i < 0 \text{ and } z_1 = 0$$

Using the above methodology (with the assumption of finite buffer), the authors in [23], proved experimentally (comparing the analytical model versus trace-driven simulation) that the C-DAR(1) model provides accurate queueing results (mean cell loss rate, mean queue length) and, therefore, is suitable for theoretical analysis of videoconference traffic. In their analysis, they used the Gamma density with parameters derived from the MOM method and an autocorrelation decay rate chosen equal to 0.9846. Taking into consideration the above, it is evident that our modeling approach with the Gamma density parameters calculated from the MOM, $K=0$ or 3 models and ACF decay rate values chosen close and higher than 0.98 (see Table 2—λ_1 values) will lead to conservative (asymptotically tight though) queueing results.

To prove our above claims we present experimental queueing results comparing the complementary distribution of the buffer overflow given by the C-DAR(1) Markov chain as derived from the calculation of (9) and (11) for any value of buffer threshold B (versus the one given by a discrete-event simulation [30] using the actual traces (trace-driven simulation [31]). For the modelling case of experiment 1—trace of terminal JP, the complementary buffer size densities from the results of the fluid flow method for all the examined PDF models (MOM, LVMAX, C-LVMAX, $K=0$ and 3) and the corresponding sample (derived from the trace-driven simulation) are plotted together (see Fig. 8). The probabilities values are always assigned at the logarithmic scale. The traffic intensity was chosen equal to 0.9[8], the autocorrelation decay rate equal to 0.9972 (from Table 2—Exp 1—λ_1 value—JP) and the number of states of

[8] Experiments with lower traffic intensities (equal to 0.8 and 0.7) were held and similar modeling results were remarked.

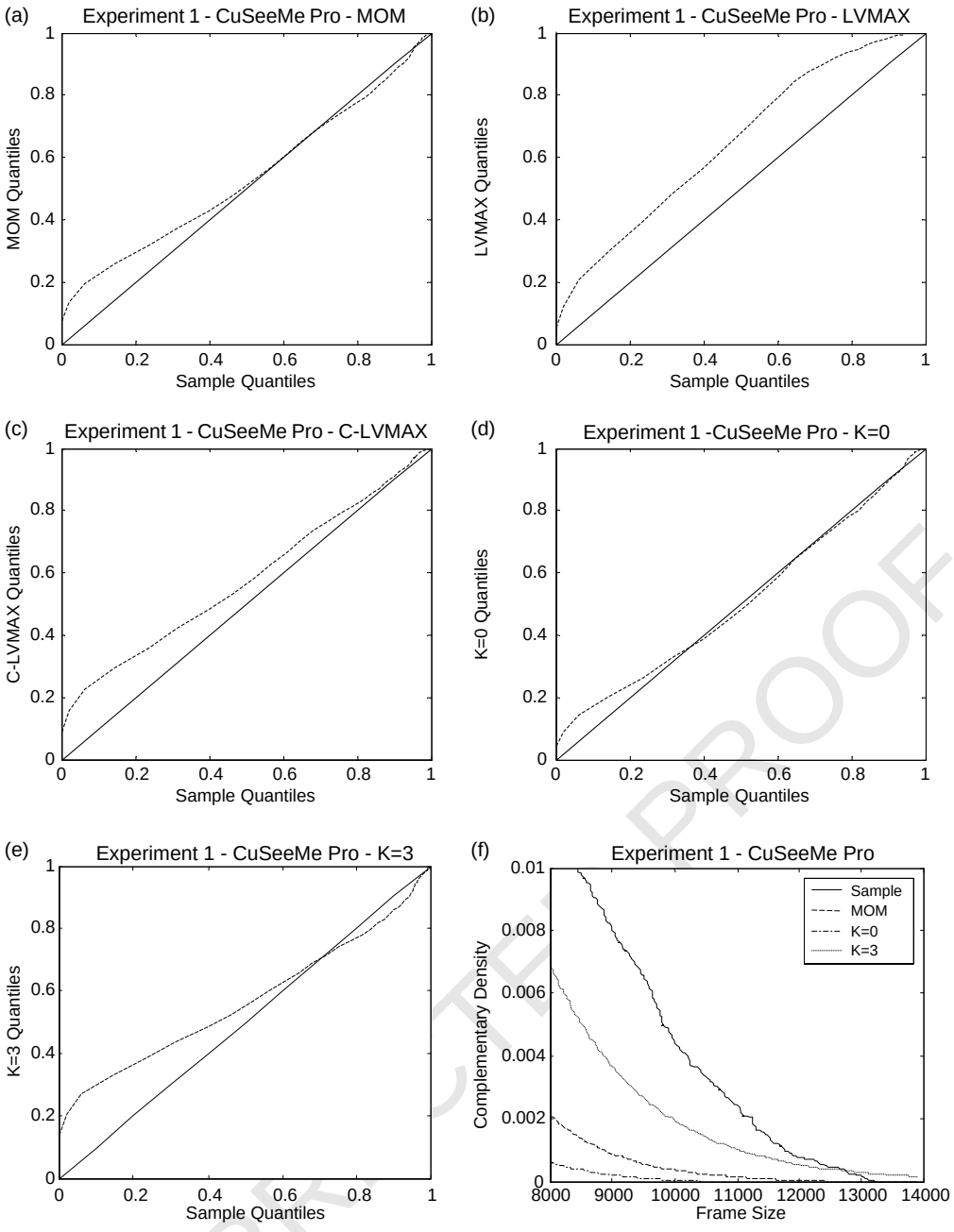

Fig. 7. Frame size histograms-Gamma models, Q–Q plots and complementary probability functions for terminal CU.

the Markov chain N equal to 10. A similar experiment was conducted for the trace of terminal CuSeeMe in experiment 3 with traffic intensity equal to 0.9, $N=10$ and $\lambda_1=0.9782$ (from Table 2—Exp 3—λ_1 value—CU).

From the consistent evidence of the results of Fig. 8, it is clear that our claims are confirmed. It is clearly indicated that the tail dominance of a model is a critical aspect with respect to its performance in queueing experiments. Both Fig. 8(a) and (b) show that the models LVMAX and C-LVMAX were optimistic in their buffer overflow estimations while the MOM, $K=0$ and 3 provided approximately tight or conservative estimations[9]. Concerning the Fig. 8(a) and (b), we have to notice that the slower decay of the analytically tractable models is physical as with the fluid-flow method the discreteness of the buffer occupancy is neglected. From the above, it becomes clear that the modeling evaluation with cumulative and complementary Q–Q plots provide valuable information for the

[9] It is obvious that a less conservative or shorter range (e.g. first 50 lags) choice of the ACF decay rate ρ would lead to more optimistic queueing results.

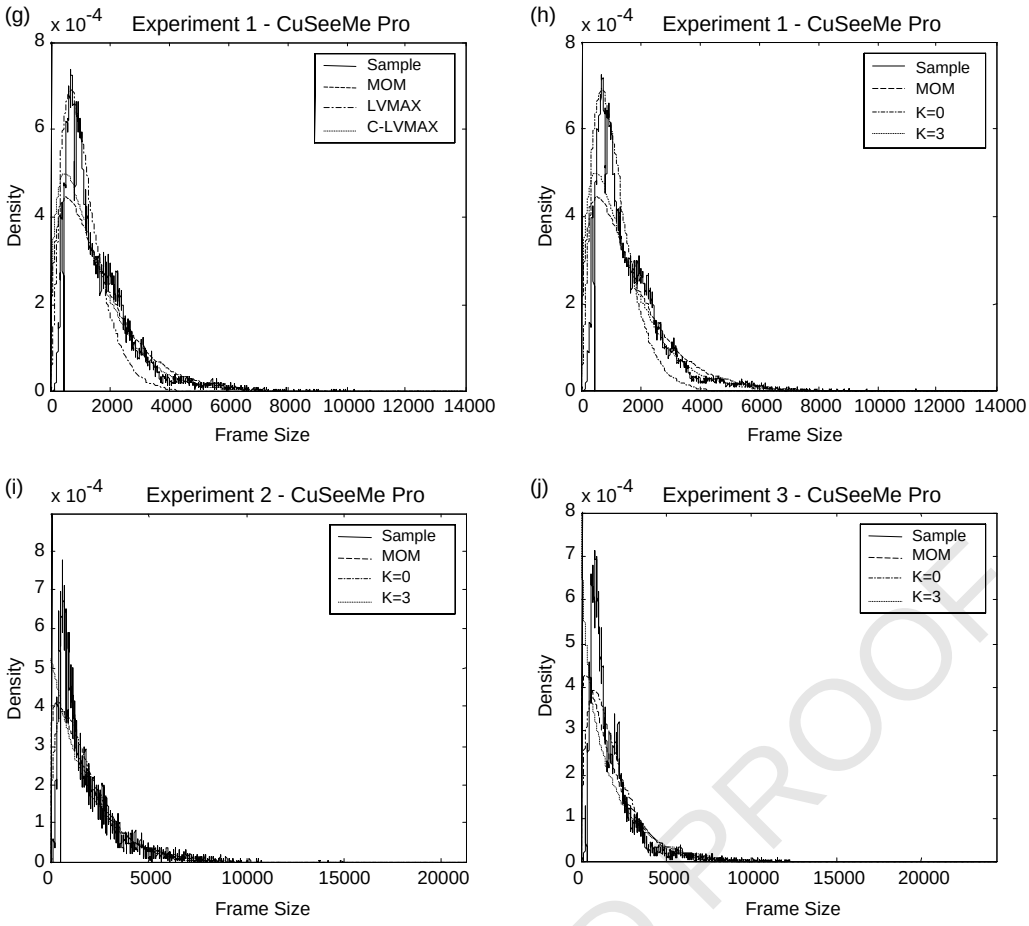

Fig. 7 (*continued*)

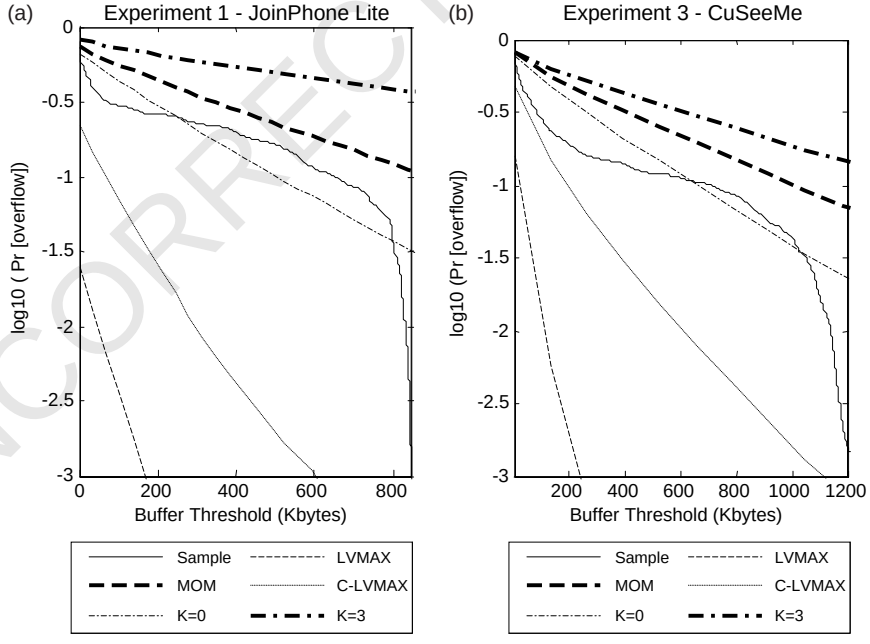

Fig. 8. Complementary buffer overflow density plots of C-DAR(1) models versus sample simulation.

queueing performance of a model. For instance, it is clear that the tail-dominance conclusions of Fig. 3(f) for terminal JP in experiment 1 reflect the results presented in Fig. 8(a).

4. Conclusions

This manuscript is a modeling assessment of H.263-encoded traffic in multipoint videoconference sessions over IP Networks. The modeling results showed that H.263 terminal traffic was stationary and seemed to possess a rapidly decaying autocorrelation function and a Gamma-formed marginal distribution. Realistic experiments with terminals using a different implementation of the H.263 codec that joined sessions with different parameters (frame rate, video bit rate) were held. The extensive analysis of the video traffic from the terminals to the MCU indicated that although the experiment parameters influence the traffic pattern, generic, though unconvential, models can capture conservatively their statistical trends. Although the correlations of H.263 traffic were found to be more complex than a simple geometric term, a careful choice of the decay rate allows the construction of a conservative approximation for queueing analysis. The modeling of the frame sizes distribution indicated that from the queueing point of view three models MOM, $K=0$ and 3 can be applied for all cases. Especially, the $K=3$ model was found to meet the requirement of tail-dominance in most cases and as a result is a good solution for the conservative application of the DAR(1) and C-DAR(1) models in queueing studies. It becomes clear that a network administrator could chose among the given models depending on the strictness of the admission control algorithm or traffic policy needed.

Further study will include queueing and simulation study of the discussed models in new experiments with various combinations of scenarios, visual content and H.263 implementations. The study of the traffic produced by the MCU in 'continuous presence' (H.263-encoded) is also a subject of future research.

Acknowledgements

The authors would like to thank Dr K. Kontovasilis for his constructive comments on improving this work.

References

[1] C. Skianis, K. Kontovasilis, A. Drigas, M. Moatsos, Measurement and statistical analysis of asymmetric multipoint videoconference traffic in IP networks, Telecommun. Syst. 23 (1) (2003) 95–122.

[2] H.S. Chin, J.W. Goodge, R. Griffiths, D.J. Parish, Statistics of video signals for viewphone-type pictures, IEEE JSAC 7 (5) (1989) 826–832.

[3] D.M. Cohen, D.P. Heyman, Performance modeling of video teleconferencing in ATM networks, IEEE Trans. Circuits Syst. Video Technol. 3 (6) (1993) 408–422.

[4] K. Dolzer, W. Payer, On aggregation strategies for multimedia traffic, Proceedings of the First Polish–German Teletraffic Symposium, Dresden, 2000.

[5] D.P. Heyman, The GBAR source model for VBR videoconferences, IEEE/ACM Trans. Networking 5 (1997) 554–560.

[6] M.R. Frater, J.F. Arnold, P. Tan, A new statistical model for traffic generated by VBR coders for television on the broadband ISDN, IEEE Trans. Circuits Syst. Video Technol. 4 (1994) 521–526.

[7] A. Erramilli, O. Narayan, W. Willinger, Experimental queueing analysis with long-range dependent packet traffic, IEEE/ACM Trans. Networking 4 (2) (1996) 209–223.

[8] Video Coding for low bit rate communication, Recommendation H.263, Article number E13923 (1998).

[9] P.A. Jacosb, P.A.W. Lewis, Time series generated by mixtures, J. Time Series Anal. 4 (1) (1983) 19–36.

[10] G. Sisodia, L. Guan, M. Hedley, S. De, A new modeling approach of H.263+ VBR coded video sources in ATM networks, RealTimeImg 6 (5) (2000) 347–357.

[11] W.C. Poon, T. Lo, A refined version of M/G/∞ processes for modeling VBR video traffic, Comput. Commun. 24 (11) (2001) 1105–1114.

[12] A. Neumaier, T. Schneider, Estimation of parameters and eigenmodes of multivariate autoregressive models, ACM Trans. Math. Software (TOMS) Arch. 7 (1) (2001) 27–57.

[13] D.P. Heyman, A. Tabatabai, T.V. Lakshman, Statistical analysis and simulation study of video teleconference traffic in ATM networks, IEEE Trans. Circuits Syst. Video Technol. 2 (1) (1992) 49–59.

[14] L. Yan-ling, W. Peng, W. Wei-ling, A Steady Source Model for VBR Video Conferences, International Conference on Information Technology: Computers and Communications, IEEE Las Vegas, Nevada, 2003 p. 268.

[15] A.A. Alheraish, S.A. Alshebeili, AR-based quadratic modeling for GOP MPEG-encoded video traffic in ATM networks, Comput. Commun. (in press), corrected proof.

[16] R. Kishimoto, Y. Ogata, F. Inumaru, Generation interval distribution characteristics of packetized variable rate video coding data streams in an ATM network, IEEE JSAC 7 (5) (1989) 833–841.

[17] S.J. Yoo, S.D. Kim, A new multi-level statistical model for variable bit rate MPEG sources over ATM networks and its performance study, Comput. Commun. 24 (3/4) (2001) 296–307.

[18] H. Ahn, J. Kim, S. Chong, B. Kim, B.D. Choi, A video traffic model based on the shifting-level process: the effects of SRD and LRD on queueing behavior, INFOCOM (2000) 1036–1045.

[19] B. Maglaris, D. Anastassiou, P. Sen, G. Karlsson, J.D. Robbins, Performance models of statistical multiplexing in packet video communications, IEEE Trans. Commun. 36 (7) (1988) 834–843.

[20] F. Fitzek, M. Reisslein, MPEG-4 and H.263 video traces for network performance evaluation, IEEE Network 15 (6) (2001) 40–54.

[21] M. Nomura, T. Fujii, N. Ohta, Basic characteristics of variable rate video coding in ATM environment, IEEE JSAC 7 (5) (1989) 752–760.

[22] D.P. Wiens, J. Cheng, N.C. Beaulieu, A class of moments estimators for the two-parameter Gamma family, Pak. J. Statist. 19 (1) (2003) 129–141.

[23] S. Xu, Z. Huang, Y. Yao, An analytically tractable model for video conference traffic, IEEE Trans, Circuits Syst. Video Technol. 10 (1) (2000) 63–67.

[24] N.D. Doulamis, A.D. Doulamis, G.E. Konstantoulakis, G.I. Stassinopoulos, Efficient modeling of VBR MPEG-1 coded video sources, CirSysVideo 10 (1) (2000) 93.

[25] D.R. Cox, H.D. Miller, The Theory of Stochastic Processes, Chapman and Hall, London, 1965.

[26] B. Ryu, Modeling and simulation of broadband satellite networks. Part II. Traffic modeling, IEEE Commun. (1999).
[27] D. Mitra, Stochastic theory of a fluid model of producers and consumers coupled by a buffer, Adv. Appl. Prob. 20 (1988) 646–676.
[28] D. Anick, D. Mitra, M.M. Sondhi, Stohastic theory of a data handling system with multiple sources, Bell Syst. Tech. J. 61 (8) (1974) 10–18.
[29] T.E. Stern, A.I. Elwalid, Analysis of separable Markov-modulated rate models for information-handling systems, Adv. Appl. Probab. 23 (1) (1991) 105–139.
[30] M. Law, W.D. Kelton, Simulation Modeling and Analysis, third ed, McGraw-Hill Higher Education, New York, 1999.
[31] F. Fitzek, P. Seeling, M. Reisslein, Using Network Simulators with Video Traces (2003), http://kom.aau.dk/∼ff/documents/tracesim.pdf.